8.1 Introduction

Dimeric or gemini surfactants have attracted much attention due to their novel properties and improved performances over their conventional surfactant [1,2]. Gemini surfactants are made up of two amphiphilic moieties attached at the level of the headgroups by a spacer group of varied nature [3-6]. Owing to their wide range of applications [7-9], various research groups are interested in designing of new type of aqueous gemini surfactant systems in order to understand their modified solution behavior [10-12]. The formation and transition of supramolecular aggregates have been greatly dependent on delicate balance of electrostatic, van der Waals, hydrophobic and steric interaction forces. Studies were also made [13-16] to elucidate the weak interactions which advance the comprehension and control of the aggregation processes. It is well known that aqueous surfactant self-assembly (*e.g.* spherical micelle) converts to higher order aggregate upon addition of salts [17,20]. The salt counterion reduces the electrostatic interaction between the headgroups, thus reducing the a_0 and thereby facilitating micellar growth [21]. Entanglement of the grown micelles into a transient network results viscoelasticity to the surfactant solutions, similar to polymers [22]. However, wormlike micelles are always in dynamic equilibrium with lower order aggregates or monomers, and thus they are also called equilibrium polymers or living polymers [23]. Such micellar systems have special applications such as paints, cosmetics, fracturing fluids in oil production [24], drag reduction [25], and enhanced oil recovery [26].

As extensively reported, addition of organic additives can also promote [12, 14, 21, 27-30] the formation of higher order aggregates by modifying some of the above mentioned interaction forces. Addition of long chain alcohols increases the aggregation number [31, 32] of the mixed micelle. Alcohols are also reported to partition themselves between micelle and background solution [33]. The micelle bound portion intercalates between charged headgroups and decreases the surface charge density [32]. The chain length and structure of the organic additive can influence the growth processes [34]. The increase in viscosity attributes to the formation of wormlike micelle, and the decrease is due to the decrease in average micellar size or due to the formation of other morphologies such as vesicles. The microstructure of the micelle can be correlated to the R_p [35] which is a rough indicator for the formation of various supramolecular assemblies. R_p is affected by an additive (salt or organic additive) in the solution. Vesicles are aggregates of surfactant bilayers entrapping large volume of water, find variety of applications [36-39]. Morphological transitions with increasing additive concentration have been studied in the past for a variety of surfactant –additive systems [23, 40-42]. Effect of addition of C_6OH has also been studied with a cationic gemini surfactant [43]. However, synergistic effect of two additives (salt and alcohol) on self-assembled system has not been studied much [44].

The temperature induced viscosity increase is another important observation which has not found much attention [14, 44, 45]. To our surprise, such synergistic effect with gemini surfactants has not been reported previously. There are some key questions that need to be addressed in order to properly understand the rationale behind the observed behavior: why viscosity increases and decreases with continuous addition of an organic additive; what type of morphology exists in samples having nearly equal viscosity; why some samples got viscous on heating; what are the morphologies in such heated systems; and how site of solubilization of an organic additive play a role in deciding the overall morphology. Keeping this view in mind, a detailed study on morphological transitions in a gemini surfactant (16-4-16) + KBr and C_6OH system, using rheology, DLS, ^1H NMR, POM and cryo- TEM has been undertaken. η_0 has provided various ranges of C_6OH concentration (hence forth represented as $[C_6OH]$) under which different microstructures coexist. DLS and NMR data support the rheology results while POM and cryo-TEM, provide direct imaging of the aggregates. Cryo-TEM is particularly suitable for visualization of microstructures of the size scale of micelles [46]. A particular advantage of cryo-TEM for studying transitions of micellar morphology is that the coexistence of many different assemblies can be directly visualized whereas an ambiguity is always associated with the data collected from other techniques.

8.2 Results and Discussion

It has been reported that addition of KBr to 30 mM 16-4-16 solution causes viscosity increase which may be due to nonspherical aggregates [47,48]. The focus of the study was to know effectiveness of the organic additives in changing the viscosity of the solution. Based on the viscosity data micellar growth was proposed due to the combined presence of KBr and medium chain alcohol. However, a lower concentration of 16-4-16 (10 mM fixed all through) has been used to produce similar systems using C_6OH. Visually, 10 mM 16-4-16+ 10 mM KBr aqueous system is clear and low viscous which transfers to clear viscous (which can trap bubble) followed by stable bluish turbid solution (no phase separation) on continuous addition of C_6OH. This observation (Figure 1) clearly suggests that a rich variety of micellar morphology is present at various concentrations of C_6OH [49]. Subsequently, a dramatic viscosity increase was observed when some of the samples were heated. These preliminary observations prompted to carry out a systematic investigation over a range of [C_6OH] and temperature.

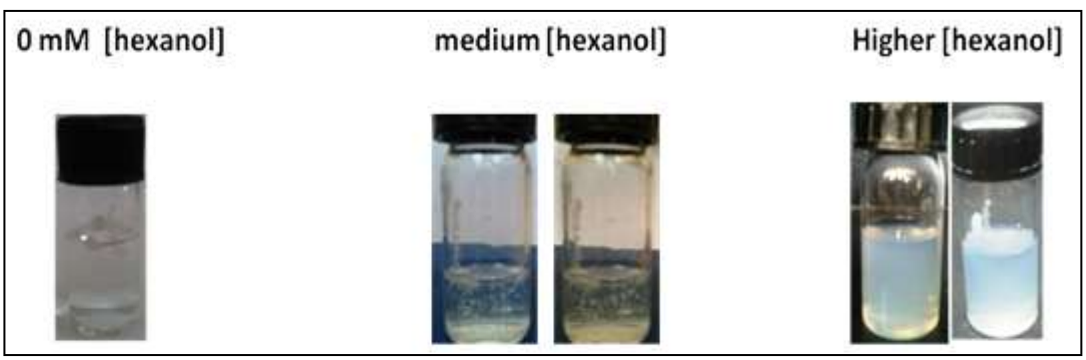

Figure 1 Visual appearance of aqueous solutions of equimolar mixtures of 16 – 4 – 16 + KBr and various [hexanol].

Figure 2 shows the variation of η_0 of 10 mM 16-4-16+ 10 mM KBr (fixed) as a function of [C_6OH]. The increase in η_0 implies that C_6OH induces the growth of the micelles and is responsible for various morphologies in different concentration ranges (regions I-III). η_0 reaches a peak (region II) and thereafter drops followed by constancy (region III) at higher [C_6OH]. Similar viscosity peaks are believed to signify morphological transitions [14, 16, 43-45, 50, 51]. It has been proposed that an additive which is surface active to a hydrocarbon-water interface will be mainly solubilized at the headgroup region and will promote structural transition. C_6OH is expected to be intercalated between 16-4-16 monomers of the micelle. This embedding of C_6OH may increase the volume of the micelle which is equivalent to an increase in the volume of the surfactant monomer. These factors increase the R_p [35], and are responsible for the uni-dimensional growth and hence viscosity increase observed in region I (Figure 2). When micelles are sufficiently long they convert more flexible wormlike micelles (in region II) which can flow comparatively easily, and hence a level off in the η_0 vs [C_6OH] plot is observed. A steep fall in η_0 (and appearance of bluish color) indicates a transition to a new morphology (region III). A decrease in η_0 and the bluishness of the system are hinting to another morphological transition.

The observed η_0 decrease at higher [C_6OH] is not easy to understand. This observation has been specifically addressed earlier in terms of formation of swollen micelles in similar surfactant systems [52, 53, 54]. Some results have also been reported for disklike aggregates present in lyotropic nematic phases observed in the phase study of potassium laurate- $C_{10}OH$- water system [53]. SANS study showed that [surfactant] was higher in the rim of the disk than in its interior, the opposite was holding good for $C_{10}OH$. The C_6OH, when present in sufficient amount, may then be supposed to get solubilized both in the palisade layer and in the interior. This discussion suggests that similar segregation is likely to occur in the present case at higher [C_6OH]. However, in a recent study it has been shown that different morphologies are present in similar conditions with C_8OH [44]. Therefore, morphology present at higher [alcohol] in surfactant systems is still a point of debate even in the present time. The studies included in following paragraphs would clear the hazy picture of the present problem about various morphologies in surfactant-salt- alcohol system.

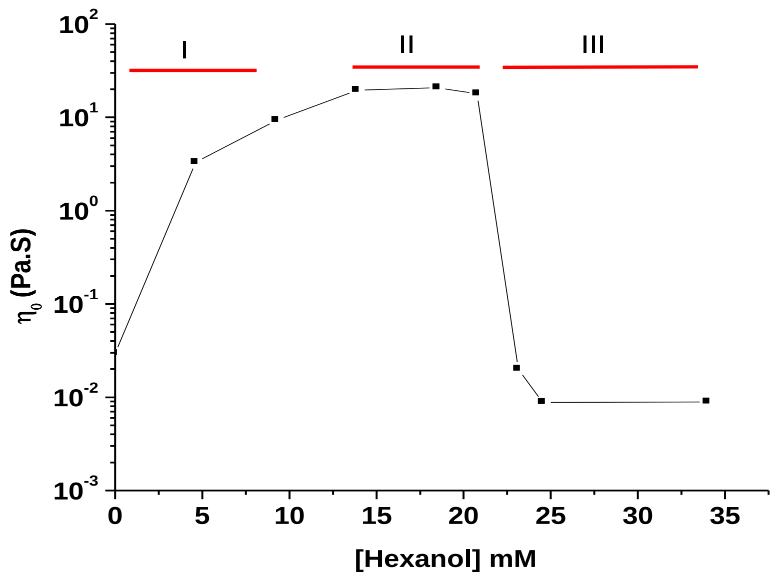

Figure 2: Variation of η_0 of aqueous 10 mM 16-4-16 + 10 mM KBr with varying concentration of C_6OH at 30 $^{\circ}$C.

The rheological response of the 16-4-16 - KBr system at various [C_6OH] is shown in Figure 3. In absence of C_6OH, sample exhibits nearly Newtonian behavior suggesting that the micelles are quite small (ellipsoids, short rods, or spheres). At relatively lower [C_6OH] (region I) sample (4.62 mM) shows a plateau in the shear viscosity at low shear rate followed by a shear thinning at higher shear rate. This rheological behavior of shear thinning can be correlated to worm like micelles in the solution. At high shear rates the viscosity drops rapidly for the breakage of worm like micelles. However, samples from region III show independence of viscosity with shear rate again. Further, this sample appears bluish in color (Figure1). These observations allow to propose the presence of vesicles in the region III. Similar rheological changes have been explained in terms of micelle to vesicle transition in various surfactants - additive systems [14, 44, 55, 56]. The transition from an ordered state to a disordered one [57] or from a higher ordered state to a lower one [45, 58, 59], (*e.g.* vesicle to micelle) on rising the temperature usually occurs among surfactant organized assembly. Therefore, temperature can play an important role which can tune such transitions. To establish the role of temperature, a few samples (containing different amounts of C_6OH) from region III chosen and performed rheological measurements. Though, these samples belong to the same region but responded to temperature in a different way.

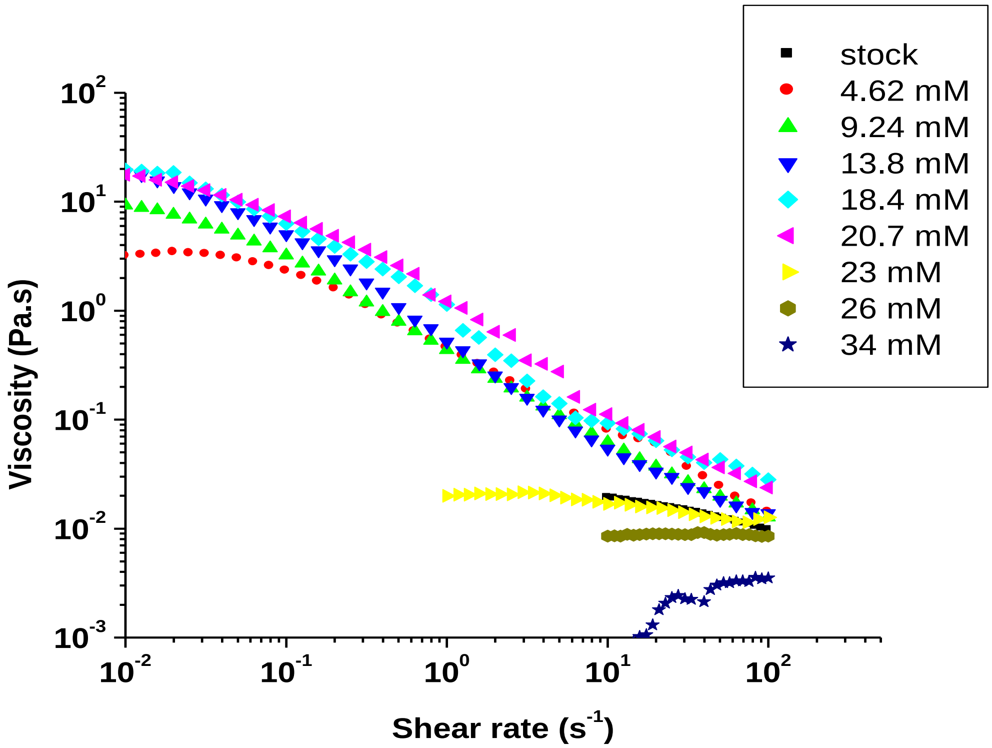

Figure 3: Variation of shear viscosity of aqueous 10 mM 16-4-16 + 10 mM KBr with shear rate for different fixed concentrations of C_6OH at 30 $^{\circ}$C.

Figure 4a shows the rheological response with temperature for 23 mM C_6OH. At lower temperature (30 or 36 $^{\circ}$C), the sample viscosity is nearly shear independent indicating that vesicles [14] are present in the solution as mentioned in region III (Figure 2). However, when the above sample heated further, the shear response has been changed showing both plateau region and shear thinning behavior. The η_0 increases three orders of magnitude with increasing temperature (Figure 4b). This novel behavior was observed relatively at much lower [surfactant] than reported for other similar surfactant systems [14, 43, 44]. The rheological response suggests about the reverse morphological transition at higher temperature.

(a)

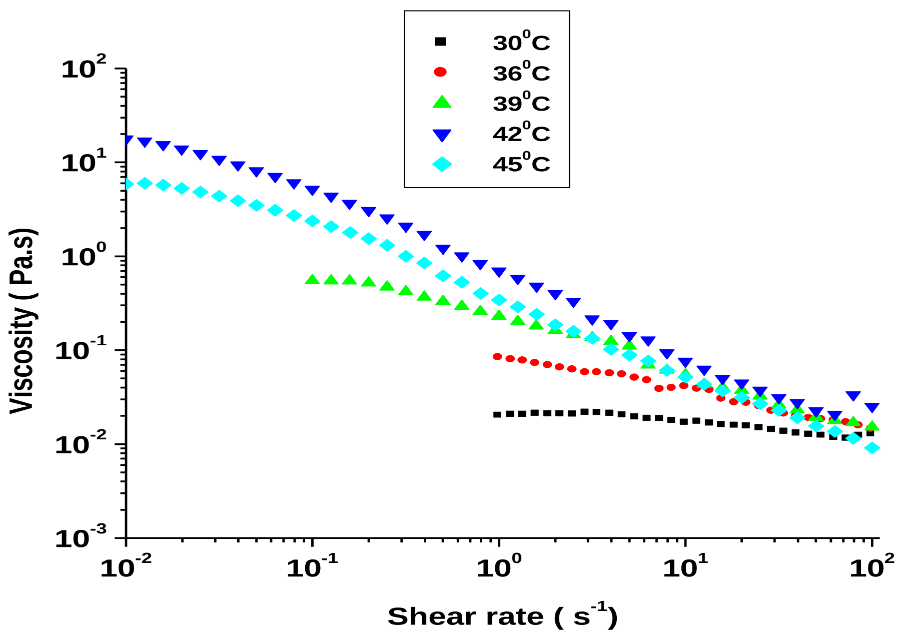

(b)

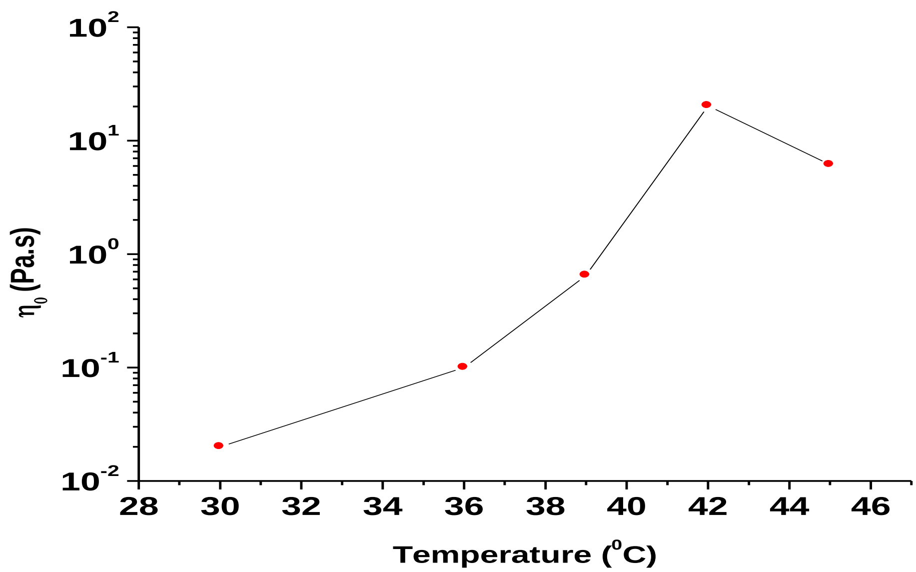

Figure 4: Variation of **(a)** viscosity with shear rate **(b)** η_0 with temperature, for aqueous 10 mM 16-4-16 + 10 mM KBr + 23 mM C_6OH.

Similar temperature effect was also performed with 26 mM C_6OH (Figure 5). Here, the plateau viscosity was not increased much indicating that the structures are stable for this composition and showing less thermal response.

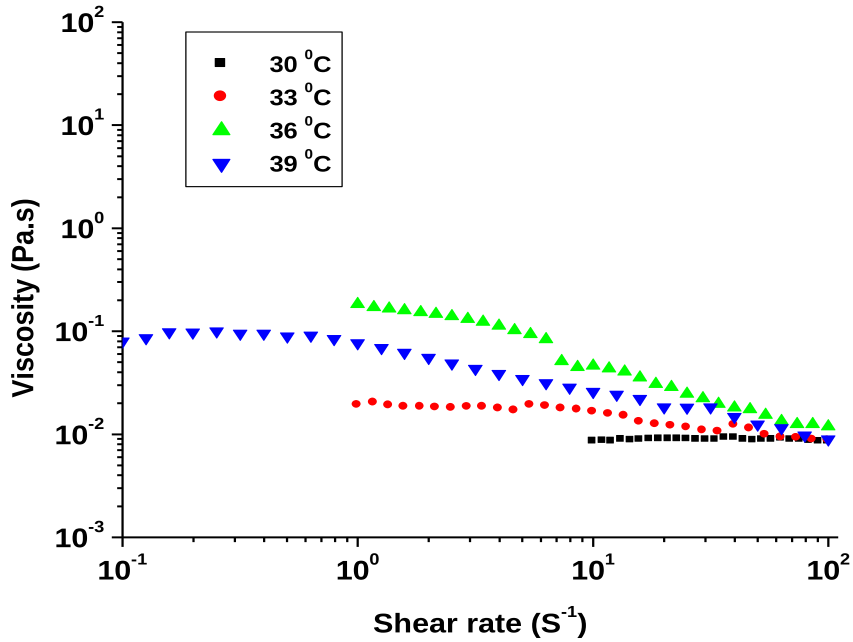

Figure 5: Variation of shear viscosity of aqueous 10 mM 16-4-16 + 10 mM KBr + 26 mM C_6OH with shear rate with different temperature.

When similar temperature effect was seen with 34 mM C_6OH, the shear response of the sample was dramatically changed (Figure 6). A distinct shear-thickening feature was also evident in the viscosity curve in addition to non-Newtonian behavior. It has been well documented that micellar growth or flow alignment of rod-shaped micelles was responsible for the shear-thickening behavior in surfactant solutions [13, 16, 55, 60-63]. The data in Figure 6 clearly indicate that rod shaped micelles are the major aggregates which coexist with a few vesicles in the system (as confirmed by POM and cryo-TEM, *supravide*). DLS results [Figure 7] were very much complementary to the η_0 data shown in Figure 2. The temperature effect was studied for the selected samples, from region II and from region III. An interesting feature has been observed in the DLS data shown in Figure 7. The sample from region II showed a decrease in

D_h with temperature, whereas D_h was found to increase for the samples from region III. Increase in D_h with increasing temperature indicate the presence of grown micelles in the system. This again corroborates the rheology data (Figures 2- 4).

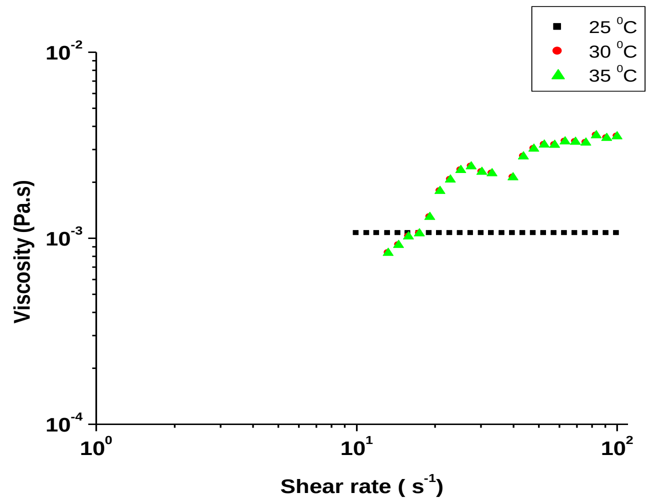

Figure 6: Variation of shear viscosity of aqueous 10 mM 16-4-16 + 10 mM KBr + 34 mM C_6OH with shear rate with different temperature.

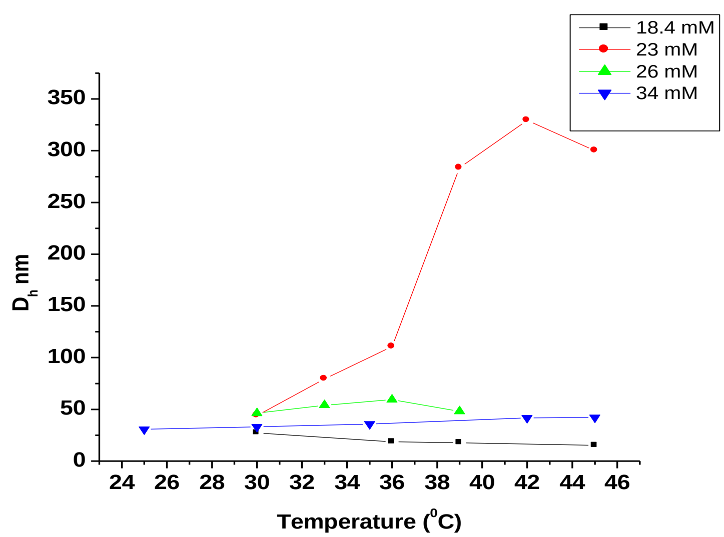

Figure 7: Size distribution profile of aggregates of aqueous 10 mM 16-4-16 + 10 mM KBr with different concentration of C_6OH with different temperatures (A) 18.4 mM(B) 23 mM (C) 26 mM (D) 34 mM.

To reveal the variations in the morphology of micellar aggregates [64] ^{1}H NMR technique has regularly been used. Figure 8 shows the NMR spectra of pure 10 mM 16-4-16, 10 mM 16-4-16+ 10 mM KBr. The labeling of hydrogen atoms of 16-4-16 is shown in Figure 8. A distinct peak broadening is observed with the addition of 10 mM KBr indicating that micellar morphology changed even in presence of KBr which is consistent with rheological data. However, addition of C_6OH causes appearance of a new peak indicating the change in environment around headgroup and chain protons. As it has been mentioned earlier, C_6OH embedded between surfactant monomers due to hydrophobic interactions with a concomitant change in palisade layer environment. On increasing the [C_6OH], decrease in peak intensity as well as broadening of a few peaks indicate further morphological transition. The probable reason of the peak broadening and disappearance is that the motion of the surfactant molecules is highly restricted in the higher order aggregate [65, 66]. Micellar growth results the slowdown of fast local motion of the segments (accompanying rod-shaped micelle) because of increase in the intra-molecular magnetic dipole-dipole interactions. The growth reduces the relaxation rate due to the slower motions of the chains (*e.g.* segmental motions or rotations of the rod-like micelles as a whole), thereby broadening of the peak takes place [16, 30, 41, 67]. Recently, line broadening has also been reported for the existence of vesicles in the solution [40, 68]. The line broadening data have been interpreted in the light of three factors, (i) various curvatures of the multiply bilayer vesicles,(ii) the polydisperse distribution and (iii) due to liquid-crystal-like nature in the aggregate interior.

A few samples are selected to study temperature effect (region III) using ^{1}H NMR. (representative NMR data for 34 mM C_6OH are given in Figure 9). Surprisingly, temperature behaves oppositely what it was observed for [C_6OH] effect. The ^{1}H NMR data (Figures 8 and 9) allowed to propose that higher order aggregates are converting to lower ones (probably vesicle to rod shaped micelle transition). This may be due to increase in partitioning of C_6OH between micellar headgroup region to that of micellar interior. Micellar headgroup partitioning has been reported to promote the formation of rod shaped micelles [21, 52].

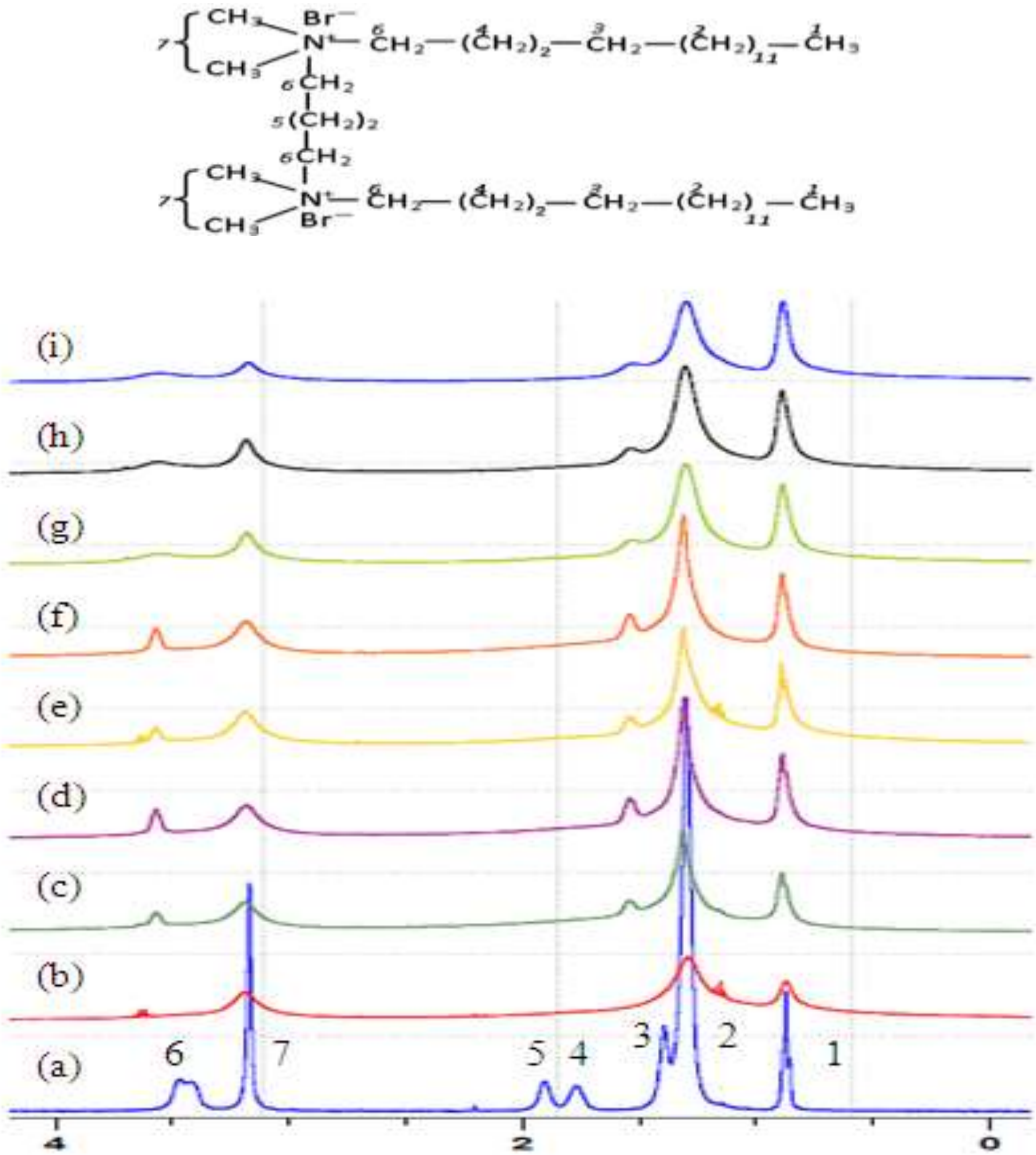

Figure 8 ^{1}H NMR spectra of aqueous 10 mM 16-4-16 + 10 mM KBr with various C_6OH concentrations; (a) pure 10 mM 16-4-16 (b) 10 mM 16-4-16 + 10 mM KBr (c) 10 mM 16-4-16 + 10 mM KBr + 9.2 mM C_6OH (d) 10 mM 16-4-16 + 10 mM KBr + 13.8 mM C_6OH (e) 10 mM 16-4-16 + 10 mM KBr + 18.4 mM C_6OH (f) 10 mM 16-4-16 + 10 mM KBr + 20.7 mM C_6OH (g) 10 mM 16-4-16 + 10 mM KBr + 23.0 mM C_6OH (h) 10 mM 16-4-16 + 10 mM KBr + 26 mM C_6OH (i) 10 mM 16-4-16 + 10 mM KBr + 34 mM C_6OH at 30 $^{\circ}$C.

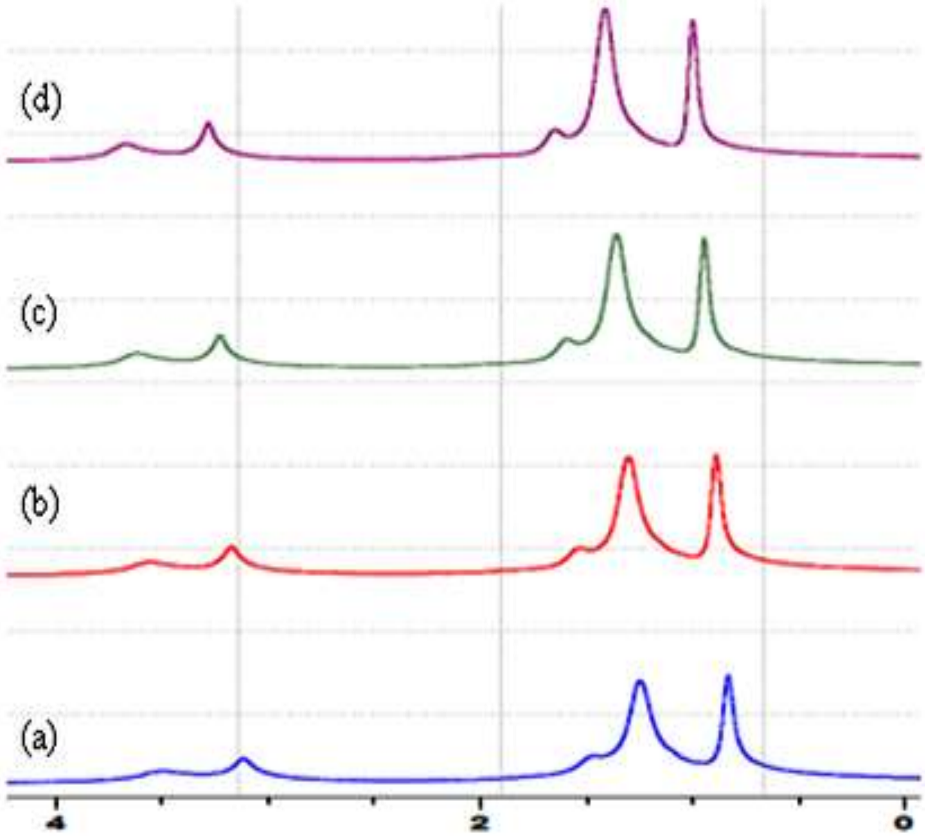

Figure 9 ^{1}H NMR spectra of aqueous 10 mM 16-4-16 + 10 mM KBr + 34 mM C_6OH with various temperature (a) 25 $^{\circ}C$ (b) 30 $^{\circ}C$ (c) 35 $^{\circ}C$ (d) 45 $^{\circ}C$.

Figure 10 (**a**, **b** and **c)** shows optical micrographs of three different concentrations of C_6OH (23, 26 and 34 mM) added to 10 mM 16-4-16 + 10 mM KBr. In all cases, one can observe a dense dispersion of polydisperse vesicles. However, small aggregates can not be seen in these optical micrographs. But presence of vesicles confirms our proposition for the morphology of region III.

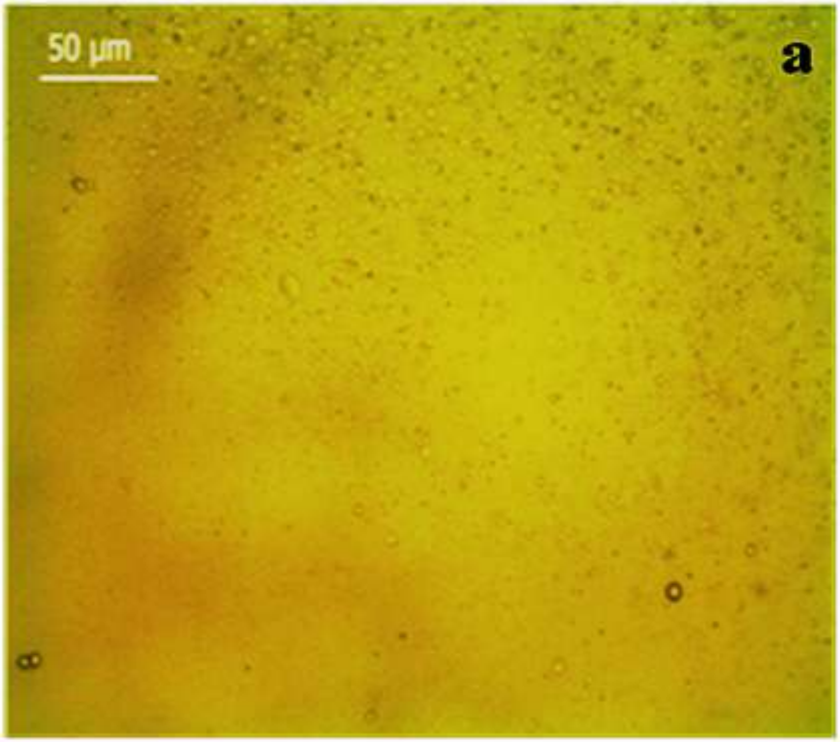
50 µm
a

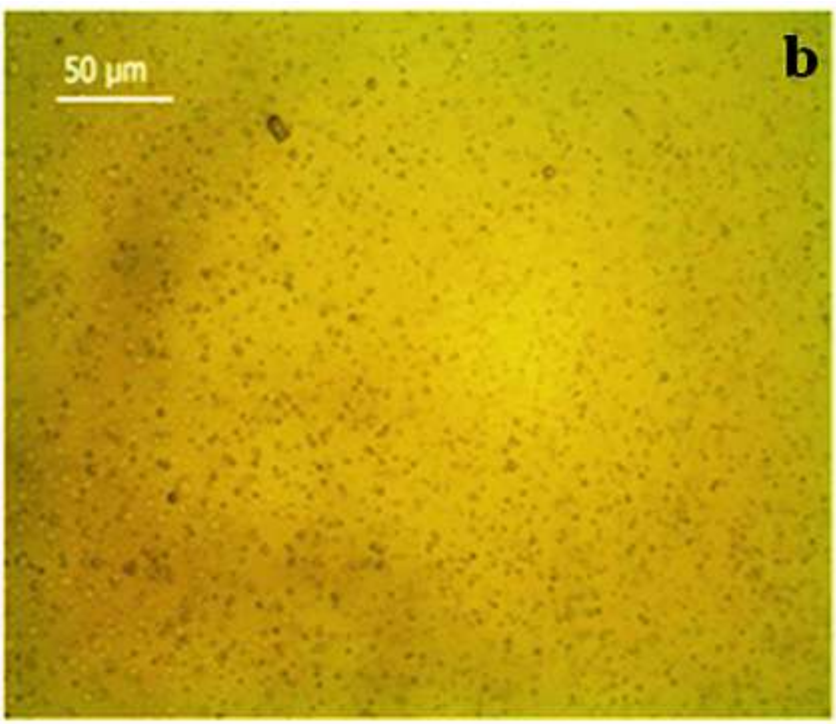
50 µm
b

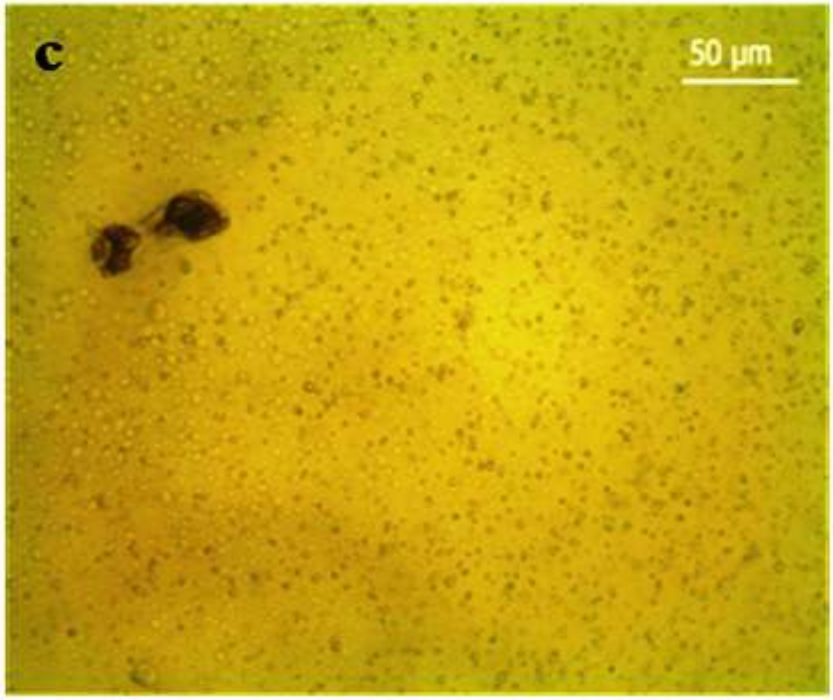

Figure 10: Optical micrographs showing the presence of vesicles in aqueous 10 mM 16-4-16 + 10 mM KBr with various C_6OH concentration (a) 23 mM (b) 26 mM (c) 34 mM 30 $^{\circ}$C.

The cryo –TEM images of the micellar aggregates in the sample containing 10 mM 16-4-16 + 10 mM KBr + 34 mM C_6OH at different temperatures (25, 35 and 45 $^{\circ}$C) are shown in Figure 11 (**a**, **b** and **c**). The images observed here clearly show temperature induced morphological transitions. Figure 11**a** shows closed ring structures in the sample. However, rheological measurements on the same sample (Figure 4) show Newtonian nature. This indicates that spherical micelles (or short rods), vesicles, or closed ring structures can give similar rheological response. The cryo-TEM data suggest that a few morphologies or their mixtures can result shear independent viscosity. Therefore, rheological data interpreted in the past should be verified by direct imaging techniques before proposing morphology in the system. The same sample at 35 $^{\circ}$C (Figure 11**b**) shows the distinct presence of vesicles together with other morphology (rod or worm like micelles). The cryo-TEM data clearly corroborate rheological results (Figure 4) where it has been proposed that mixture of two morphologies exists at 35 $^{\circ}$C. Analysis of the micrographs shows the complexity of the present mixed micelle system, including polydisperse vesicles with respect to size and shape. The cryo-TEM micrograph at 45 °C (Figure 11**c**) shows the formation of dense wormlike micelles in the solution. Therefore, cryo-TEM images together with other data demonstrate that various morphological transitions can be realized only by simple variation of [C_6OH] and temperature.

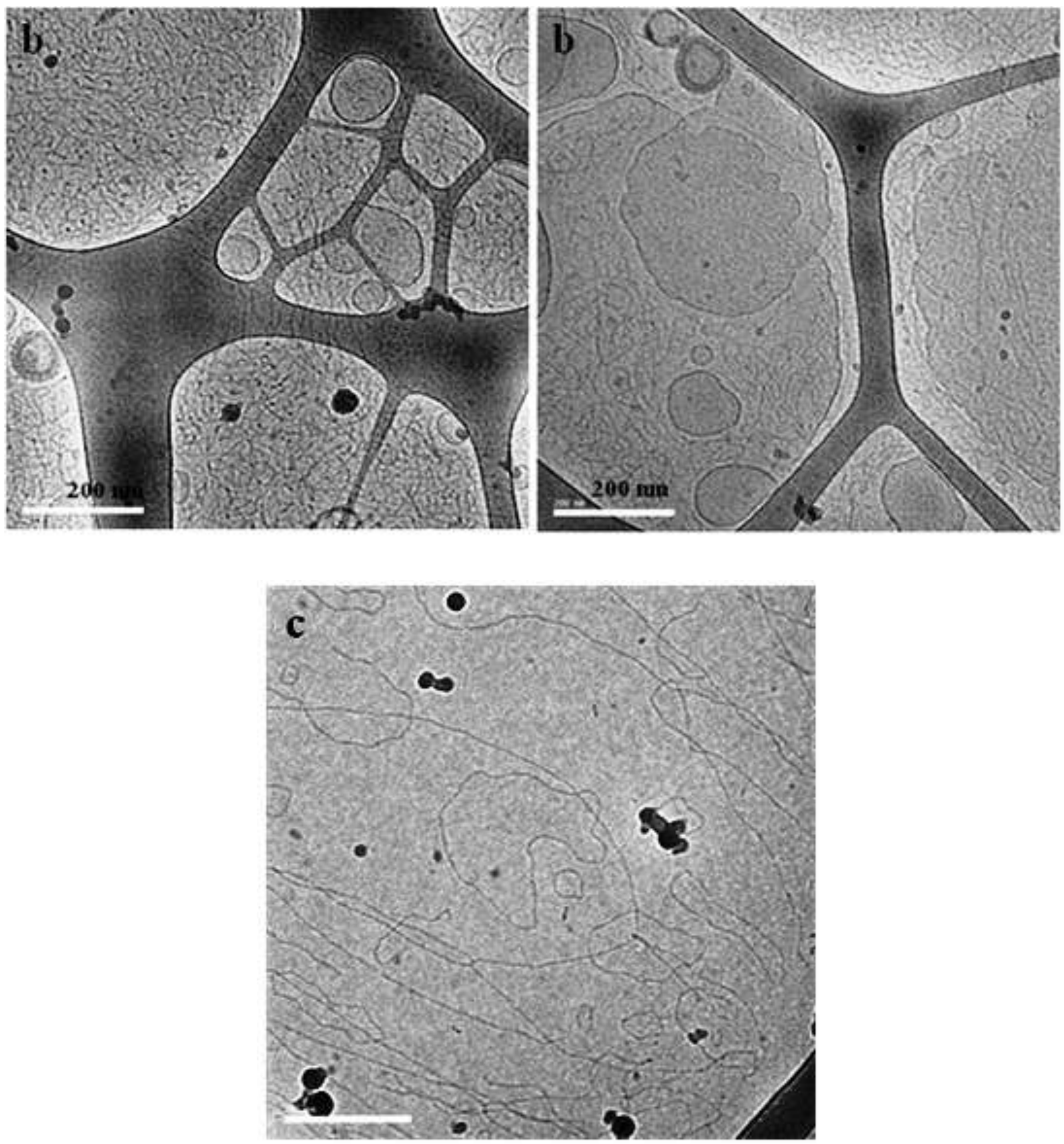

Figure 11: Cryo-TEM micrographs showing the presence of different morphology in aqueous10 mM 16-4-16 + 10 mM KBr + 34 mM C_6OH with different temperature (a) 25 °C (b) 35 °C (c) 45 °C.

8.2.1Mechanism for morphological transition

It is expected that ellipsoidal or short rod micelles are formed initially (10 mM 16-4-16 +10 mM KBr). Initially, C_6OH has been solubilized in the headgroup region. Such medium chain alcohols are preferably embedded between monomers comprising a micelle. Due to this C_6OH penetration in a surfactant-rich film (between the similarly charged head groups), the head group repulsion is minimized. As a result, a_0 decreases and consequently R_P increases. An increase in R_P could be understood by considering a 16-s-16 + C_6OH couple as a single-surfactant. Hence, the volume of the micellar core will increase because of above penetration which is equivalent to increasing v [27]. Thus, adding low amounts of C_6OH promotes the growth of micelles into wormlike aggregates. However, when [C_6OH] is increased, sufficient amount of C_6OH would be solubilized in the interior region in addition to the headgroup region. Due to this internal solubilization, the headgroup area could be further reduced and effective monomer volume (v) is also increases resulting the formation of low -curvature aggregates (*i.e.* vesicles). The partitioning of C_6OH may be affected by the increase in temperature with a concomitant release of bound Br^- ions. In region III, a sufficient amount of C_6OH is present (*e.g.* 34 mM) which will be embedded between the headgroups. In this situation temperature increase may release bound Br^- towards background solution. To compensate the increased electrostatic interactions, C_6OH would prefer the headgroup region again (the probable sites of C_6OH partitioning in a micellar solution can be (i) bulk solution, (ii) headgroup region and (iii) interior region [33, 52]) and may initiate the formation of rodlike micelles. This indeed was observed from rheological and cryo-TEM data (Figures 4 and 11). A schematic mechanism of above morphological transitions is depicted in scheme 1.

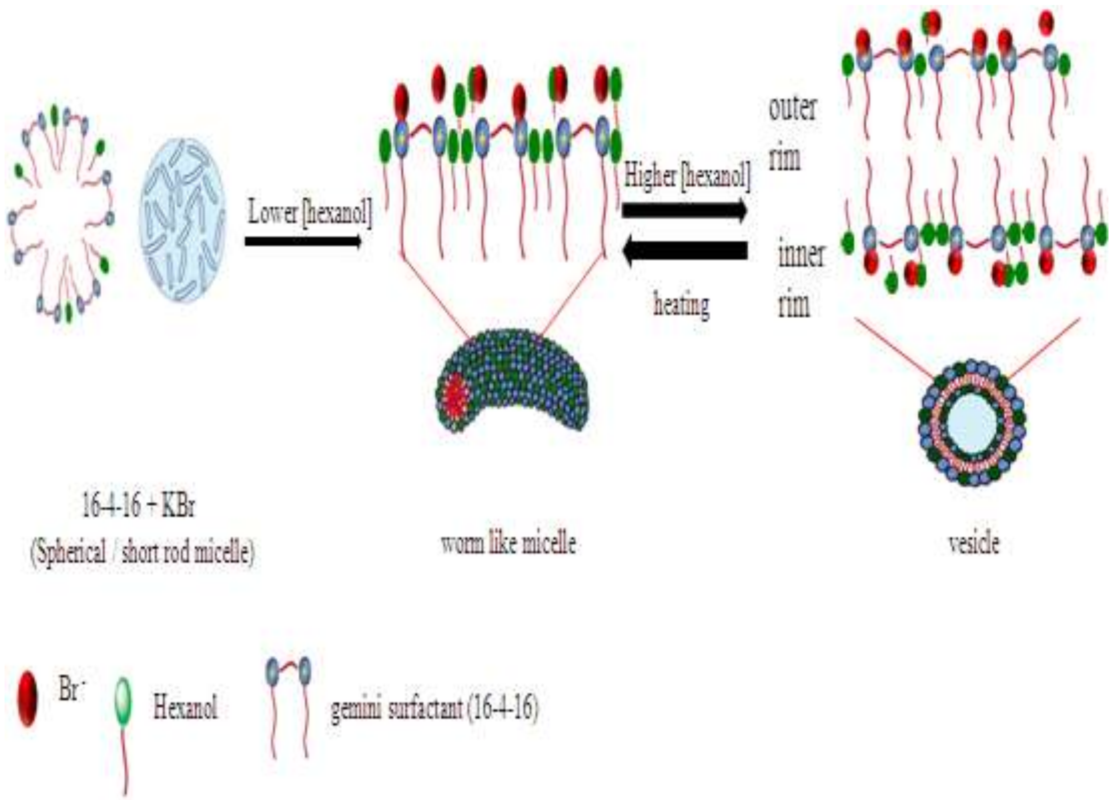

Scheme 1 Mechanism of the morphological transition in 16-4-16 - KBr - C_6OH system.

8.3 Conclusions

[C_6OH] and temperature compensate each other for the solution viscosity (especially in region III). Various morphological transitions are taking place on continuous addition of C_6OH (region I-III). Vesicle can be one of the additives when the effective [C_6OH] in the aggregate interior is higher. At higher temperature this interior C_6OH may prefer to go towards headgroup region with concomitant change vesicles into wormlike morphology.

References

1) F. M. Menger, J.S. Keiper, *Angew. Chem. Intern. Ed.* 39 (2000) 1906.
2) R. Zana, *Adv. Colloid Interface Sci.* 97 (2002) 205, and references therein.
3) R. Zana, *Curr. Opin. Colloid Interface Sci.*1 (1996) 566.
4) S. Ikeda, In: Raoul Zana, R., Xia, J. (eds.), *Gemini surfactants: Synthesis, interfacial and solution-phase behavior, and applications*. CRC Press, 2003.
5) R. Zana, M. Benrraou, R. Rueff, *Langmuir* 17(1991) 1072.
6) Y.S Wang, R. Guo, J.Q. Xi, *J. Colloid Interface Sci.* 331(2009) 470.
7) M. J. Rosen, *Chem. Technol.* 23 (1993) 30.
8) M. N. Maithufi, D. J. Joubert, B. Klumperman, *Energy Fuels* 25 (2011) 162.
9) A. J. Kirby, P. Camilleri, J. B. F. N. Engberts, M. C. Feiters, R. J. M. Nolte, O. Soderman, M. Bergsma, P. C Bell, M. L Fielden, C. L. G. Rodriguez, P. Guedat, A. Kremer, C. McGregor, C. Perrin, Ronsin G, M. C. P. Van Eijk, *Angew. Chem. Intern. Ed.* 42 (2003)1448.
10) R. Zana, M. In, H. Levy, G. Duportail, *Langmuir* 13 (1997) 5552.
11) M. In, V. Bec, O. Aguerre-Chariol, R. Zana, *Langmuir* 16 (2000) 141.
12) P. Baglioni, E. Braccalenti, E. Carretti, R. Germani, L. Goracci, G. Savelli, M. Tiecco, *Langmuir* 25 (2009) 5467.
13) H. Yin, Z. Zhou, J. Huang, R. Zheng, Y. Zhang, *Angew. Chem. Intern. Ed.* 42 (2003) 2188.
14) T. S. Davies, A. M. Ketner, S. R. Raghavan, *J. Am. Chem. Soc.* 128 (2006) 6669.
15) S. Kumar, H. Patel, S. R. Patil, *Colloid Polym. Sci.* 291(2013) 2069.
16) S. Kumar, H. Patel, *J. Mol. Liquids* 190 (2014) 74.
17) A. Sein, J. B. N. F Engberts, *Langmuir* 11(1995) 455.
18) S. Kumar, N. Parveen, Kabir-ud-Din, *J. Phys. Chem. B* 104 (2004) 9588.
19) K. D. Collins, G. W. Neilson, J. E. Enderby, *Biophysical chemistry* 128 (2007) 95.
20) N. Vlachy, B. C. Jagoda, R. Vacha, D. Touraud, P. Jungwirth, W. Kunz, *Adv. Colloid Interface Sci.* 146 (2009) 42.
21) S. Kumar, D. Bansal, Kabir-ud-Din, *Langmuir* 15 (1999) 4960.

22) S. R. Raghavan, E. W. Kaler, *Langmuir* 17 (2001) 300.

23) L. Wattebled, A. Laschewsky, *Langmuir* 23 (2007) 10044.

24) J. Yang, *Curr. Opin. Colloid Interface Sci.* 7 (2002) 276.

25) H. Rehage, H. Hoffmann, *Rheol. Acta* 21 (1982) 561.

26) G. C. Maitland,*Curr. Opin. Colloid Interface Sci.* 5 (2000) 301.

27) Z. Lin, J. J. Cai, L. E Scriven, H. T. Davis, *J. Phys. Chem.* 98 (1994) 5984.

28) A. M. Ketner, R. Kumar,T. S. Davies, P. W. Elder, S. R. Raghavan, *J. Am. Chem. Soc.* 129 (2007)1553.

29) Kabir-ud-Din, W. Fatma , Z. A. Khan, A. A. Dar, *J. Phys. Chem. B* 111 (2007) 8860.

30) W. C. Zhang, G. Z. Li, J. H. Mu, L. Q. Zheng, *J. Dispersion Science and Technology* 21 (2000) 605.

31) M. Almgren, J. E. Lofroth, *J. Colloid Interface Sci.* 81(1981) 486.

32) P. Lianos, J. Lang, C. Strazielle, R. Zana, *J. Phys. Chem.* 86 (1982) 1019.

33) D. Mukerjee, Mittal K. L., Ed.; *In Solution Chemistry of surfactants*; Plenum Press: New York, 1979, p.193

34) J. Karayil, S. Kumar, P. A. Hassan,Y. Talmon, L. Sreejith, *RSC Adv.*5 (2015) 12434.

35) J. N. Israelachvili, D. J. Mitchell, B.W. Ninham, *J. Chem. Soc. Faraday trans. II* 72 (1976) 1525.

36) M. J. Ostro, P. R. Cullis, *Am. J. Hosp. Pharm.* 46 (1989) 1576.

37) I. I. Yaacob, A. C. Nunes, D. O. Shah, *J. Colloid Interface Soc.* 168 (1994) 289.

38) G. Xia, L. Hua, F. Zhang, S. Zheng, R. Guoa, *J. Colloid Interface Sci.* 324 (2008) 185.

39) H. Akatsukaa, M. Yamamotoa, Y. Oharaa ,Y. Otsubob, *Colloids Surf. A* 326 (2008) 169.

40) D. Yu, X. Huang, M. Deng ,Y. Lin, L. Jiang , J. Huang, Y. Wang, *J. Phys. Chem. B* 114 (2010) 14955.

41) U. S. Siddiqui, F. Khan, I. A. Khan, A. A. Dar, Kabir-ud-Din, *J. Colloid Interface Sci* 355 (2011) 131.

42) T. Wang, J. Hu , C. Peng, H. Liu, *J. Dispersion Science and Technology* 28 (2007) 1169.
43) R. Oda, L. Bourdieu, *J. Phys. Chem.*101 (1997) 5913.
44) L. Sreejith, S. Parathakkat, S. M. Nair, S. Kumar, G. Varma , P. A. Hassan, Y. Talmon, *J. Phys. Chem. B* 115 (2011) 464.
45) P. A. Hassan, B. S. Valaulikar, C. Manohar, F. Kern, L. Bourdieu, S. J. Candau, *Langmuir* 12 (1996) 4350.
46) P. K. Vinson, J. R. Bellare, H. T. Davis, W. G. Miller, L. E. Scriven, *J. Colloid Interface Sci.* 142 (1991) 74.
47) Kabir-ud-Din, U. S. Siddiqui, S. Kumar, *Colloids and Surfaces* 301 (2007) 209.
48) U. S. Siddiqui, S. Kumar, Kabir-ud-Din, *Montash Chem.* 140 (2009) 457.
49) Hoffmann, H. In *Structure and Flow in Surfactant Solutions*; Herb, C. A., Prud'homme, R. K., Eds.; American Chemical Society: Washington, DC, 1994; pp 2-31.
50) R. Oda, I. Huc, S. J. Candau, F. C. Mackintosh, *Nature* 399 (1999) 566.
51) A. C. Kumar, H. Erothu, H. B. Bohidar, A. K. Misra, *J. Phys. Chem. B* 115 (2011) 433.
52) Kabir-ud-Din, Bansal, D.; Kumar, S. *Langmuir* 13 (1997) 5071.
53) Y. Hendrikx, J. Charvolin, M. Rawiso, *J. Colloid Interface Sci.* 100 (1984) 597.
54) P. M. Lindemutht, G. L. Bertrand, *J. Phys. Chem.* 97 (1993) 7769.
55) G. C. Kalur, S. R. Raghavan, *J. Phys. Chem. B* 109 (2005) 8599.
56) Y. Yang, J. Dong, X. Li, *J. Colloid Interface Sci.* 380 (2012) 83.
57) S. Forster,T. Plantenberg, *Angew. Chem.* 41 (2002) 712.
58) E. Mendes, R. Oda, C. Manohar, J. Narayanan, *J. Phys. Chem. B* 102 (1998) 338.
59) R. T. Buwalda, M. C. A. Staurt, J. B. F. N. Engberts, *Langmuir* 16 (2000) 6780.
60) S. Q. Wang, *J. Phys. Chem.* 94 (1990) 8381.
61) R. Bruinsma,W. Gelbart, A. B. Shaul, *J. Chem. Phys.* 96 (1992) 7710.

62) S. Hofmann, H. Hoffmann, *J. Phys. Chem. B* 102 (1998) 5614.

63) C. L. Oelschlaege, G. Waton, S. J. Candau, M. E. Cates, *Langmuir* 18 (2002) 7265.

64) J. J. Effling, I. J. McLennan, N. M. Van Os, J. C. T. Kwak, *J. Phys. Chem.* 98 (1994) 12397.

65) M. Tata, V. T. John, Y. Y Waguespack, G. L. McPherson, (1994) *J. Phys. Chem.* 98 (1994) 3809.

66) S. A. A. Rizvi, L. Shi, D. Lundberg, F. M. Menger, *Langmuir* 24 (2008) 673.

67) K. Kalyanasundaram, M. Gratzel, J. K. Thomas, *J. Am. Chem. Soc.* 97 (1975) 3915.

68) M. Villeneuve, R. Ootsu, M. Ishiwata , H. Nakahara, *J. Phys. Chem. B* 110 (2006) 17830.